Plant Soil (2024) 499:503–519
https://doi.org/10.1007/s11104-024-06475-3

RESEARCH ARTICLE

Plant growth-promoting fungi and rhizobacteria control *Fusarium* damping-off in Mason pine seedlings by impacting rhizosphere microbes and altering plant physiological pathways

Cun Yu · Jun Lv · Hongyun Xu

Received: 31 July 2023 / Accepted: 2 January 2024 / Published online: 16 January 2024

Abstract

Aims Damping-off disease, caused by *Fusarium oxysporum*, affects the growth of *Pinus massoniana* seedlings. Plant growth-promoting fungi and rhizobacteria (PGPF and PGPR) are widely used in agriculture to control plant soil-borne disease, however, the joint mechanism by which they inhibit damping-off disease in forestry requires further exploration.

Methods The current study screened for the ability of antagonistic PGPF and PGPR strains to inhibit the pathogen, and used soil microbiome and plant transcriptome technologies to characterize the biocontrol mechanism.

Results PGPF strain 3Y, identified as *Trichoderma longibrachiatum*, and PGPR strain K29, identified as *Burkholderia stabilis*, were screened and found to strongly inhibit the growth of *F. oxysporum* through direct contact with the hyphae. The combined use of *T. longibrachiatum* and *B. stabilis* effectively reduced disease incidence and severity, and promoted the growth of *P. massoniana* seedlings, and enhanced soluble sugar, proline, SOD and POD activities. Compound strains treatment impacted the structure of rhizosphere bacterial microbial community, causing significant differences in the relative abundances of some key phyla and genera, promoting the enrichment of some beneficial microorganisms. Transcriptome profiles showed that combination treatment with the biocontrol strains induced the expressions of 8541 differentially expressed genes (DEGs). These genes participated in key biological pathways associated with starch and sucrose metabolism, plant hormone signal transduction, photosynthesis, antioxidant enzymes, and proline synthesis.

Conclusion The combined use of PGPF and PGPR strains controlled *F. oxysporum* infection of *P. massoniana* seedlings by regulating physiological responses and soil microbial community.

Keywords *Fusarium* disease · *Trichoderma longibrachiatum* · *Burkholderia stabilis* · Biological control · Rhizosphere microbes · Physiological pathways

Responsible Editor: Ulrike Mathesius.

Supplementary Information The online version contains supplementary material available at https://doi.org/10.1007/s11104-024-06475-3.

C. Yu (✉) · J. Lv
College of Forestry, Guizhou University, Huaxi District, Guiyang 550025, China
e-mail: chifengyucun@163.com

H. Xu
College of Eco-Environmental Engineering, Guizhou Minzu University, Guiyang 550025, China

Introduction

Pinus massoniana (*P. massoniana*) is a major pioneer tree species used for afforestation in Southern

China (Quan and Ding 2017). Damping-off disease caused by *Fusarium oxysporum* can induce extensive death of Masson pine seedlings in a short time frame (Luo and Yu 2020), restricting the cultivation, afforestation, and resource utilization of *P. massoniana.* Chemical pesticides are widely used to control infectious pathogens because they are convenient, quick-acting, and effective (Sharma et al. 2020). However, excessive dependence on their use over a long period can worsen the physical and chemical properties of soil, destroy the soil microbial community, and increase the drug resistance of pathogens (Mehmood et al. 2021). Due to their safety, durability, and ecological nature, biological control agents (BCAs) are a promising alternative to chemical pesticides to suppress infectious diseases in Pine trees (Yu and Luo 2020). There is an urgent need for BCAs in addition to the commonly used agents, *Bacillus subtilis*, *Beauveria bassiana*, *Trichoderma harzianum*, and *Paecilomyces lilacinus* (Weerapol et al. 2019; Villa-Rodriguez et al. 2022), to be identified.

Plant growth-promoting fungi (PGPFs), such as *Trichoderma* species, are widely used in agriculture to control plant disease (Jogaiah et al. 2013). *Trichoderma* spp. use several mechanisms to effectively inhibit various pathogens in Pine trees. *T. atroviride* improves the systemic tolerance of *Diplodia pinea*-infected *P. radiata* and reduces 20% of the seedling dieback (Reglinski et al. 2012). *Trichoderma* spp. from *P. sylvestris* bark can produce volatile compounds with antimicrobial activity and have typical mycoparasitic manifestations against Botryosphaeriaceae (Karlicic et al. 2021). *Trichoderma* spp. decreases morbidity associated with *Fusarium circinatum* damping-off in *P. radiata* seedlings (Morales-Rodríguez et al. 2018). Recently, *T. longibrachiatum* was shown to play a vital role in helping crops resist diseases. This fungus accumulates key metabolites, which help onion plants (*Allium cepa* L.) to resist *F. oxysporum* (Abdelrahman et al. 2016). *T. longibrachiatum* TG1 controls wheat (*Triticum aestivum L.*) crown rot disease by activating the plant defense system and increasing the transcription of pathogenesis-related genes (Boamah et al. 2021). However, there are few reports on the effect of *PGPFs* on *Fusarium* damping-off disease in *Pinus.*

Several plant growth-promoting rhizobacteria (PGPR) are effective BCAs (Wang et al. 2021b), promoting plant growth by secreting indole acetic acid and dissolving minerals, and also protecting plants from infection by inducing systemic resistance and the production of antagonistic substances (Takishita et al. 2018). The genera *Bacillus* and *Pseudomonas* are predominant PGPRs that protect various crops against pathogens, such as *V. dalhiae* and *F. oxysporum* (Beneduzi et al. 2012; Essalimi et al. 2022). More recently, *Burkholderia* spp. (*B.* spp.) have also been identified as PGPRs, showing great potential against various soil-borne pathogens (Esmaeel et al. 2020). While *B. contaminans, B. cepacia* and *B. stabilis* are shown to produce various antimicrobial metabolites against wilt and root rot diseases (Jung et al. 2018; Kim et al. 2020; Heo et al. 2022), very little research has assessed the role of *Burkholderia* spp. in disease control in *Pinus.*

Recent studies have indicated that microbial combinations can more effectively inhibit plant pathogens than a single inoculate. Elshahawy and El-Mohamedy (2019) found that the combined use of five *Trichoderma* isolates was the most effective method of suppressing damping-off and root rot by activating defense enzymes. Few studies have assessed the combined effects of PGPF and PGPR in controlling fungal disease. Many BCAs can induce systemic acquired resistance (ISR) to combat plant pathogens (Heo et al. 2022). Plant rhizosphere microbial communities are the first line of defense for protecting plants against different biological and abiotic stresses (Dini-Andreote 2020). Thus, it is important to study the disease resistance mechanism of a PGPF and PGPR combination by analyzing its effect on the rhizosphere microbial community structure and plant physiological system.

PGPF and PGPR strains were recently isolated from *P. massoniana* to assess their ability to control *Fusarium* damping-off in seedlings. The current study sought to (1) evaluate the antifungal activity of PGPFs and PGPRs against *F. oxysporum in vitro*, (2) identify the growth promotion and biocontrol effects of a PGPF and PGPR combination in *P. massoniana* seedlings, and (3) analyze changes in the soil microbial community structure and physiological system after PGPF and PGPR co-inoculation.

Materials and methods

Fungal and bacterial strains

The fungal and bacterial strains used in this study were isolated from a 20-year-old healthy Masson pine in Guiyang City, Guizhou Province (26.44°N, 106.65°E), China, in June 2019. Three fungal strains, 3Y, 6Y, and 12Y were isolated from the root and determined to be IAA-producing strains, which identified them as PGPFs (Luo 2020). Four bacterial strains, K3, K15, K25, and K29 were isolated from rhizosphere soil using a method developed by Bagyalakshmi et al. (2017) and determined to be potassium solubilization and IAA-producing, which identified them as PGPRs. The *F. oxysporum* strain (GenBank accession no. MK356552), which causes damping-off disease in seedlings, was isolated from the roots of *P. massoniana* (Luo and Yu 2020).

Determination of antagonistic activity in vitro

The dual culture technique was used to measure the antagonistic effect of different PGPF and PGPR strains against the pathogenic *F. oxysporum* strain (Bell et al. 1982). A 5 mm diameter mycelial disc from an actively growing 7-day *F. oxysporum* culture was placed on the center of each PDA plate, and a 10^8 CFU/mL bacterial suspension from each PGPR strain (K3, K15, K25, and K29) was used to draw a line 10 mm from the disc between the left and right sides. Plates inoculated with *F. oxysporum* alone were used as a control. The plates were incubated in the dark at 28 °C for 5 days. The 5 mm diameter mycelial disc of *F. oxysporum* and each PGPF strain (3Y, 6Y, and 12Y) from the 7-day-old cultures were placed across from each other (about 60 mm apart) on a 90 mm diameter PDA plate. A PDA plate inoculated with an *F. oxysporum* disc served as the control. The plates were incubated in the dark at 28℃ for 7 days.

After dual culture, the inhibition rate was calculated using the following formula: inhibition rate (%) = $([R_1 - R_2] / R_1) \times 100$ (Díaz-Gutierrez et al. 2021), where R_1 is the radial growth of the pathogen on the control plate, and R_2 is the radial growth of the pathogen on the dual culture plate. The hyphae at the contacting edge of the pathogen were collected to observe interactions using a light microscope (Olympus CX21, Tokyo, Japan). The experiment was performed with six replicates.

To measure extracellular enzyme activity (protease, cellulase, and chitinase), 2 µL suspension of the K25 and K29 strains (10^8 CFU/mL) were inoculated on detection medium containing 1.5% skim mile power (Heo et al. 2022), 1% carboxymethyl cellulose (Díaz-Gutierrez et al. 2021), and 1% colloidal chitin (Roberts and Selitrennikoff 1988). After culture at 30℃ for 5 days, the plates were assessed for the presence of a transparent halo. 3,5-Dinitrosalicylic acid (DNS) colorimetry and Folin-phenol methods was used to measure chitinase and protease activities.

Plant inoculation and treatment

The fungal strain 3Y (*Trichoderma longibrachiatum*, MT131278.1) and the bacterial strain K29 (*Burkholderia stabilis*, OR262944), identified based on their morphology and molecular sequences, were used for plant inoculation. The methods are described in detail in Method S1. A 1×10^8 CFU/mL bacterial suspension (of *B. stabilis* and 1×10^6 spores ml^{-1} spore suspensions of *T. longibrachiatum* and *F. oxysporum* were prepared. The phloem of fine roots from 3-month-old seedlings were wounded lightly with sterilized scalpels once and planted in a plastic pot (12.5 cm high, 14.5 cm upper diameter, 10.2 cm lower diameter) at three seedlings per pot. The suspension was then poured into the soil near the root using a sterilized syringe (Sofo et al. 2010). The following four treatment groups were used: (1) Fo, soil inoculated with a 5 mL *F. oxysporum* suspension (control), (2) Fo + 3Y, soil inoculated with a mixture of a 5 mL *F. oxysporum* and a 5 mL *T. longibrachiatum* suspension, (3) Fo + K29, soil inoculated with a 5 mL *F. oxysporum* and a 5 mL *B. stabilis* suspension, (4) Fo + 3Y + K29, soil inoculated with a 5 mL *F. oxysporum*, 5 mL *T. longibrachiatum*, and 5 mL *B. stabilis* suspension. Ten pots were used as a biological repeat, and each treatment included three biological repeats. After treatment, seedlings were grown at 25 ± 0.5℃ for 60 days, with 16/8 h day/night lighting and a relative humidity of 70%.

Disease and growth index measurements

After inoculation for 60 d, disease incidence (DI), disease severity (DS), and control index (CI) were

evaluated. DI was assessed using the following formula: DI (%) = (I / R) × 100 (Toghueo et al. 2016, where I is the number of infected plants, and R is the total number of plants receiving treatment. DS was determined based on the severity of symptoms, which was divided into five incidence levels (0, 1, 2, 3, and 4) (Díaz-Gutierrez et al. 2021), and evaluated using the following formula: DS (%) = (∑(A × B) /(T×M)× 100, where A is the number of diseased plants at each level, B is the corresponding incidence level, T is the total number of plants, and M is the maximum incidence level. CI was calculated using the following formula: CI (%) = ((D_1-D_2) / D_1) × 100, where D_1 is the DS value in the control (Fo treatment) and D_2 is the DS value in the corresponding treatment group. After the disease index assessment, seeding height, taproot length, and the number of lateral roots were determined. Meanwhile, above-ground shoots and roots were separately collected to assess their fresh and dry weight.

Assay of physiological indices

Physiological parameters were measured after 60 inoculations. The chlorophyll content was determined using the 80% acetone extraction method (Wood et al. 2020). The relative conductivity was determined using a conductometer (DDS-308$^+$, INESA, Shanghai, China) as described by Fan et al. (1997). Malondialdehyde (MDA), soluble sugar, and proline content were detected using the thiobarbituric acid, anthrone-sulfuric, and acidic-ninhydrin methods, respectively (Draper et al. 1993). Peroxidase (POD), superoxide dismutase (SOD), and catalase (CAT) activities were determined using the nitroblue tetrazolium photoreduction, guaiacol colorimetry, and potassium permanganate titration methods, respectively (Lin et al. 2020).

Soil genomic DNA extraction, sequencing, and data processing

After 60 days of inoculation, the rhizosphere soil samples (Fo, Fo + 3Y, Fo + K29, Fo + 3Y + K29) were collected, homogenized, and sampled for DNA extraction. Ten pots were pooled as a replicate. Three biological replicates were used for each treatment. The 16 S rDNA gene V3-V4 region of the soil bacteria and the fungus ITS1-ITS2 region were amplified using the bacteria-specific primers, 341 F (5'- CTA CGGGNGGWGCAG-3') and 805R (5'- GACTAC HVGGATCTAATCC-3'), and the fungal primers, ITS1F (5'- CTTGGTCATTTAGGAGATAAA-3') and ITS2R (5'- CTGCGTTCTTCGCGATGC-3'), respectively. Purified PCR products were sequenced using the Illumina MiSeq sequencing system (Sangon Biotech, Shanghai, China). For raw sequencing data, operational taxonomic units (OTUs) were assigned based on a 97% sequence similarity threshold, and the representative OTU classification was obtained using the QIIME (v1.8.0) and R package (v3.2.0) (Edgar 2010). The relative abundance of each phylum or genus was calculated using the following formula: relative abundance (%) = n_i/N, where n_i is the number of sequences for each OTU, i represents an individual OTU, and N is the total number of sequences for all OTUs in the sample. Alpha diversity indices (Simpson, Shannon, ACE, and Chao1) were used to access the diversity and richness of the bacterial and fungal communities, and the permutational MANOVA (ADONIS) analysis and principal component analysis (PCA) was used to evaluate differences in the community structures associated with each treatment (Tuomisto 2010).

RNA extraction, cDNA library construction, and transcriptomics analysis

After 60 days of incubation, total RNA was extracted using whole Masson Pine seedlings from the Fo and Fo + 3Y + K29 treatment groups. Six seedlings was pooled as a replicate. Three biological replicates were used for each treatment. Six high-quality cDNA libraries were created as previously described by Liu et al. (2020) and sequenced using the Illumina HiSeq 2500 system (Sangon Biotech, Shanghai, China). Raw read data were stored in the NCBI database with accession number PRJNA997741. Clean reads were identified by removing the adapter, ambiguous, and low-quality reads from the raw data. Non-redundant unigenes were obtained using the Trinity method (Grabherr et al. 2011). The transcription level of each unigene was calculated and normalized using the fragments per kilobase of transcript per million fragments mapped reads (FPKM) method (Trapnell et al. 2010). The differentially expressed genes (DEGs) in the two different treatment groups were assigned with a p-value < 0.05 and |log2 fold change (FC)| > 1

using the DEGseq package (Love et al. 2014). Significant enriched KEGG pathway was determined with a p adjusted using the Bonferroni correction (q values) ≤ 0.05.

Statistical analysis

Data were analyzed with SPSS software (IBM 21.0, New York, NY, USA) for one-way analysis of variance (ANOVA) using the Duncan test ($P \leq 0.05$) to determine significant differences.

Results

Antagonistic activity of the PGPF and PGPR strains against the pathogen, *F. oxysporum*

Four PGPR strains, K3, K15, K25, and K29, were used for the antagonistic activity measurements. All four strains prevented the growth of *F. oxysporum*, with inhibition rates ranging from 35.00 to 55.67%. Of these, K25 and K29 had the strongest inhibition rates, reaching 50.33% and 55.67% respectively (Fig. 1A, B). In the dual culture conditions, K25 and K29 had significant inhibitory effects on the growth of *F. oxysporum* mycelium, causing breakage, bending, shrinking, and deformity (Fig. 1C). K29 strain solubilized skim milk and colloidal chitin by forming a halo zone on the agar, indicating that this strain had chitinase activity and was able to secrete proteases, while the K25 strain had protease activity (Fig. S1A). The proteases and chitinase activities of K29 strain were significantly higher than that of K25 strain (Fig. S1B). The growth of the three PGPF strains, 3Y, 6Y, and 12Y, against *F. oxysporum* are shown in Fig. 2. The 3Y strain strongly prevented *F. oxysporum* growth (Fig. 2A), with an inhibition rate of 75% (Fig. 2B). Microscopic examination showed that the mycelium of *F. oxysporum* became curled and deformed after co-cultivation with the 3Y strain (Fig. 2C). Based on these results, the K29 and 3Y strains were chosen for subsequent experiments.

Characterization of the K29 and 3Y strains

The K29 strain was identified based on its cell and colony morphology, biochemical and physiological

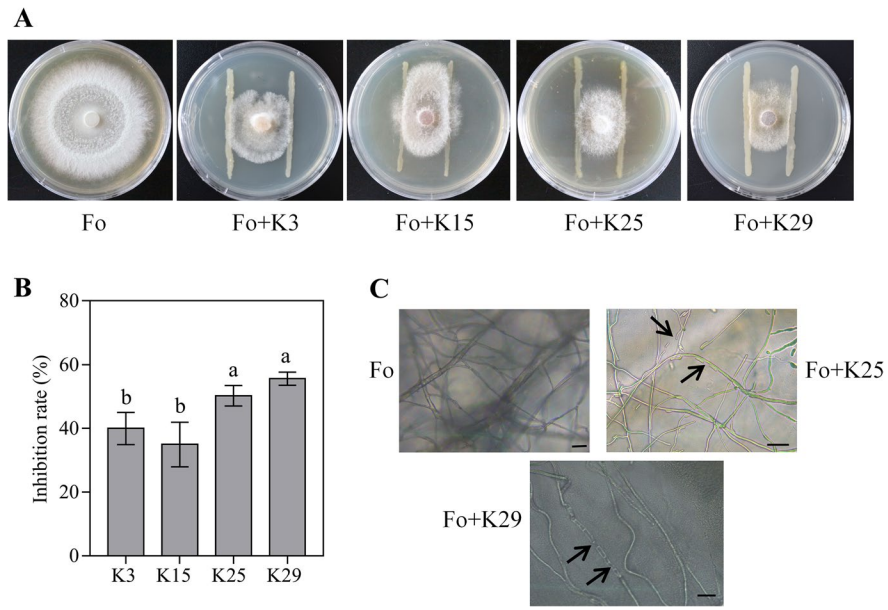

Fig. 1 Antagonistic activity of PGPR strains against *F. oxysporum*. **A** Dual cultures inoculated with *F. oxysporum* as a control (Fo), K3 strain against *F.oxysporum* (Fo + K3), K15 strain against *F. oxysporum* (Fo + K15), K25 strain against *F.oxysporum* (Fo + K25), K29 strain against *F.oxysporum* (Fo + K29). **B** Inhibition rate of the four PGPR strains against *F. oxysporum* in dual culture, different letters on the bars indicate significant differences at $P \leq 0.05$ according to Duncan's multiple range test. **C** Observation of *F. oxysporum* mycelium in dual culture after 5 days, Scale bars = 20 μm

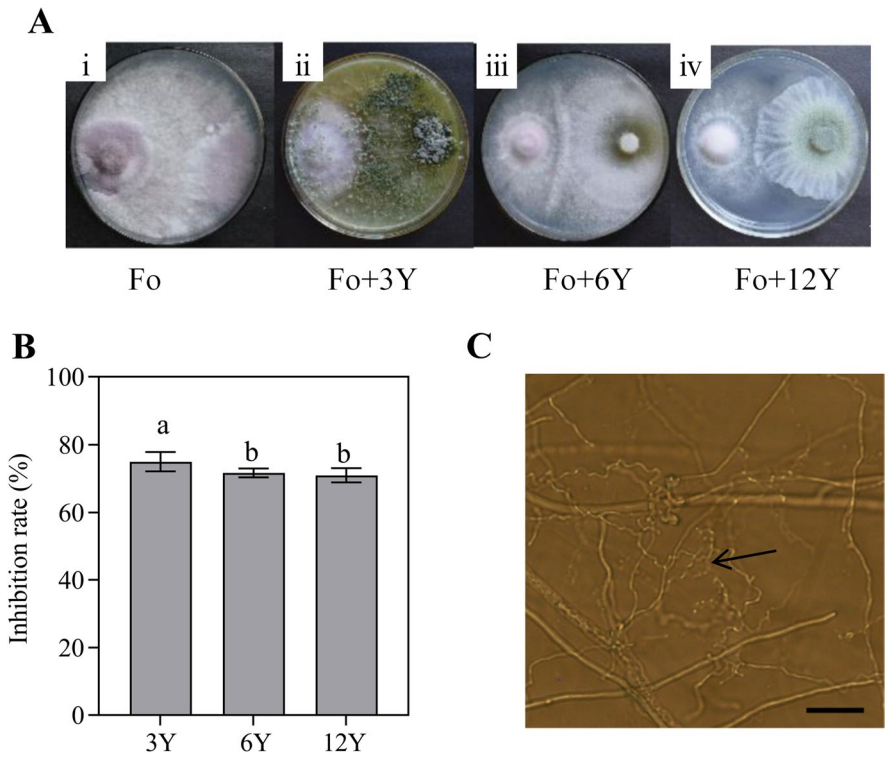

Fig. 2 Antagonistic activity of PGPF strains against *F. oxysporum*. **A** Dual cultures inoculated with *F. oxysporum* as a control (i, Fo), 3Y strain against *F. oxysporum* (ii, Fo + 3Y), 6Y strain against *F. oxysporum* (iii, Fo + 6Y), 12Y strain against *F. oxysporum* (iv, Fo + 12Y). **B** Inhibition rate of the PGPF strains against *F. oxysporum* in dual culture. The different lower-case letters indicate significant difference at $P \leq 0.05$ according to Duncan's multiple range test. **C** Observation of mycelial interactions between 3Y strain and *F. oxysporum* after 7 days in dual culture, scale bars = 20 μm

test results, and 16s rRNA gene sequence. Under a scanning electron microscope, cells of the K29 strain were short and rod-shaped, approximately 0.7–0.9 μm in length and 0.2–0.3 μm in width (Fig. 3A). The colonies had a milky white color with a moist surface, protrusions, no wrinkles, and fast growth (Table S1). The K29 strain was Gram-negative and oxidized bacteria. Amylolysis, contact enzyme, and gelatin hydrolysis test results were positive, the methyl red test (MR test) and Voges-Proskauer test (V-P test) results were negative, and the strain was able to grow at 25–35℃ with tolerance to 2% NaCl (Table S1). Based on its 16 S rDNA gene sequence, the K29 strain (OR262944) displayed the greatest sequence homology with *Burkholderia stabilis* (MG571686.1) (Fig. 3B). The upper side of the 3Y colony was yellowish green and the lower side was yellow, the colony grew rapidly and had an obvious whorl, the conidiophore had simple branches and a strong main shaft, and the conidia were oval, smooth, green, and 3.0–4.5 × 1.5–2.3 μm in size (Fig. 3C). Based on the ITS rDNA gene sequence, the 3Y strain (MT131278.1) had the highest sequence homology with *T. longibrachiatum* (MT102396.1) and formed a distinct clade from the other *Trichoderma* spp (Fig. 3D).

Biocontrol activity of combined *T. longibrachiatum* and *B. stabilis* treatment against *Fusarium* damping-off disease in *P. massoniana*

Fusarium oxysporum inoculation caused needle withering and yellowing and the symptoms were alleviated by K29 or 3Y treatment (Fig. 4A). Disease incidence and severity were significantly lower in response to Fo + K29, Fo + 3Y, and Fo + K29 + 3Y than to Fo treatment alone ($P < 0.05$, Fig. 4B, C), and K29 and 3Y together had the highest control index (Fig. 4D). The seedling height, number of lateral roots, and fresh and dry weight were significantly higher following Fo + K29 + 3Y than Fo treatment alone ($P < 0.05$, Fig. 4E-I). These results indicated that the combination of *T. longibrachiatum* and *B. stabilis* effectively reduced *Fusarium* infection and promoted seedling growth.

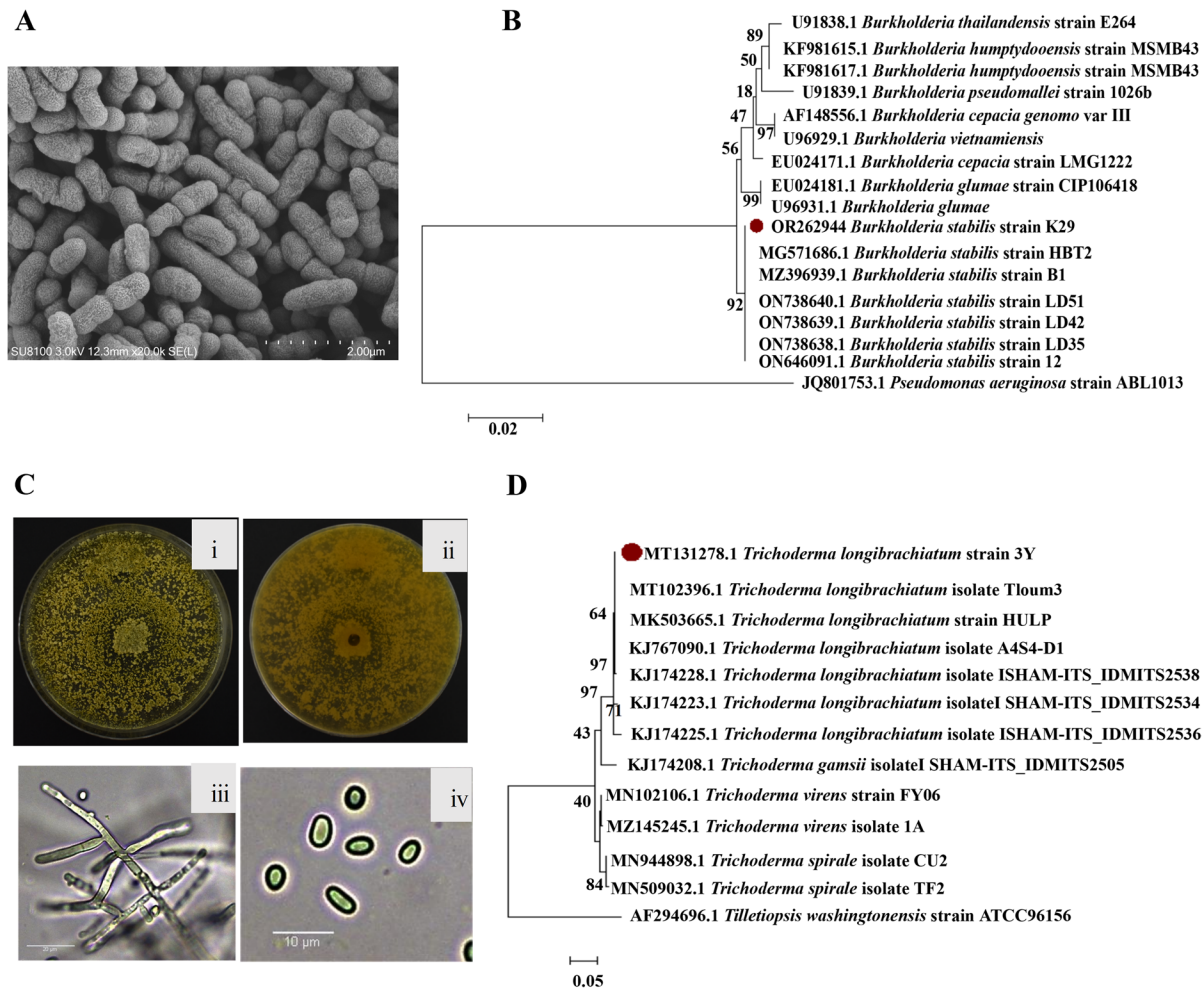

Fig. 3 Morphological and molecular identification of K29 strain as *Burkholderia stabilis* and 3Y strain as *Trichoderma longibrachiatum*. **A** Morphology observation with a scanning electron microscope. **B** Phylogenetic tree based on 16 S rDNA sequence. These 16 S rDNA sequences of related strains were downloaded from NCBI GenBank database. The tree was structured using neighbor joining (NJ) method, with the bootstrap analyses of 1000 cycles. Bar represents sequence divergence of 0.02 nucleotides. **C** Morphology observation, colonial morphology on the upper side (i) and lower side (ii) on PDA medium; microscopic observation of conidiophore (iii) and conidia (iv). **D** Phylogenetic tree based on ITS sequence

Plant physiological characteristics under different treatment conditions

The seedlings in the Fo + K29 + 3Y treatment group had a higher chlorophyll content than those in the other treatment groups (Fig. 5A). The relative conductivity and MDA content were higher in plants receiving Fo treatment and lower in seedlings inoculated with the K29 or 3Y strain (Fig. 5B, C). The soluble sugar content of the shoots and proline content of the shoots and roots were higher in the Fo + K29 + 3Y treatment group than in the other treatment groups (Fig. 5D, E). Meanwhile, the activity of antioxidant enzymes, including SOD, POD, and CAT, was significantly higher in the Fo + K29 + 3Y treatment group (Fig. 5F-H).

Analysis of rhizosphere community structure

The permutational MANOVA (ADONIS) analysis and PCA analysis indicated that there was no significant difference between Fo and Fo + 3Y + K29 treatment for fungal community ($P > 0.05$, Fig. 6A, Table S2), but there was a marked difference in the

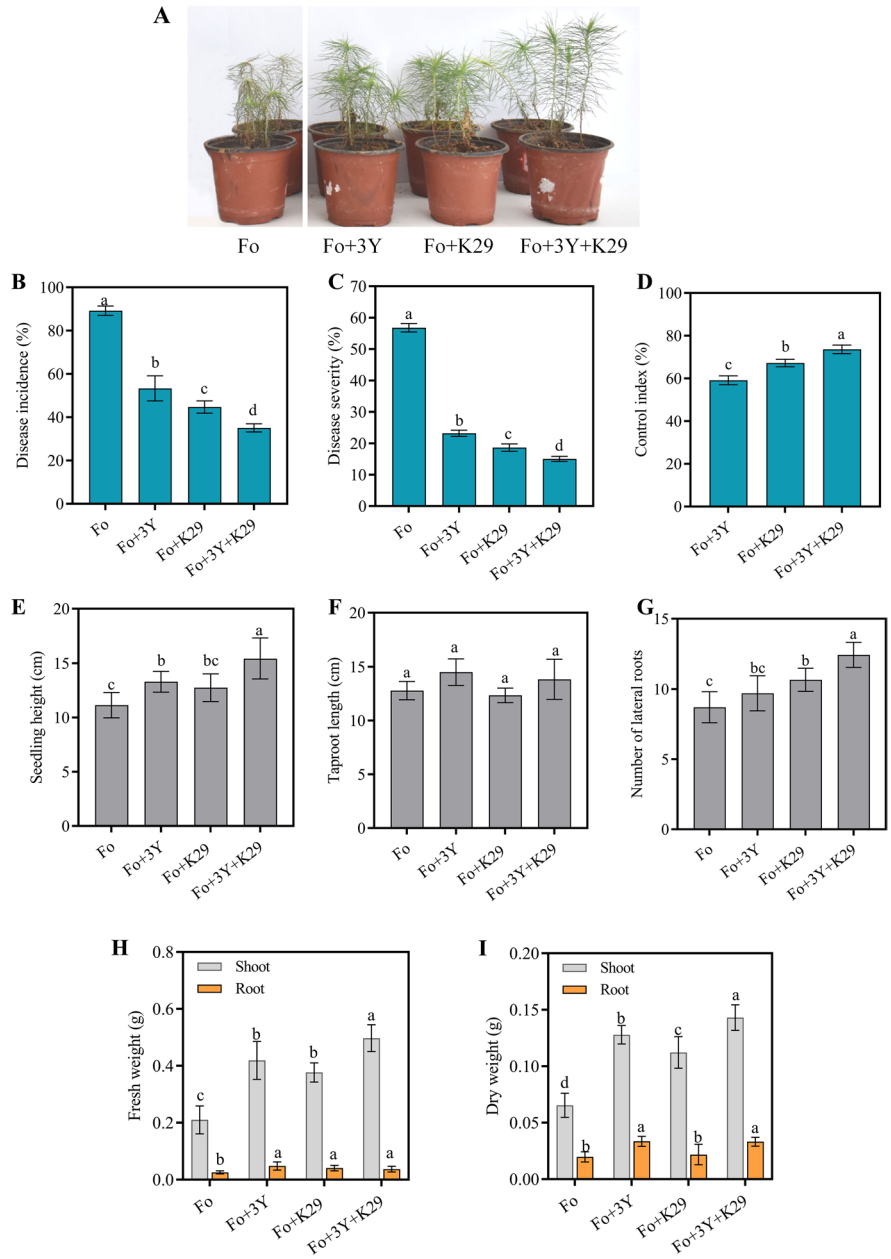

Fig. 4 The effects of different treatment groups on disease incidence and seedlings growth. **A** The representative photographs, **B** Disease incidence, **C** Disease severity, **D** Control index, **E** Seedling height, **F** Taproot length, **G** Number of lateral roots, **H** Fresh weight, **I** Dry weight. Fo, plant inoculated with *F. oxysporum*; Fo + 3Y, plant inoculated with *T. longibrachiatum* and *F. oxysporum*; Fo + K29, plant inoculated with *B. stabilis* and *F. oxysporum*; Fo + 3Y + K29, plant inoculated with *F. oxysporum*, *T. longibrachiatum* and *B. stabilis*. Treatment with different strains was used as a variable, shoot or root was analyzed separately by one-way ANOVA. Bars indicate the mean ± SE for three independent biological replicates ($n = 30$). Different letters indicate significant differences at $P \leq 0.05$

bacterial community structure of the different treatment groups ($P = 0.05$, Fig. 6B, Table S2). The Shannon index of the fungal community was significantly higher in the Fo + 3Y treatment group than in the Fo treatment group ($P < 0.05$), but there was no significant difference in the total number of OTUs or in the ACE and Chao indexes of the different treatment groups ($P > 0.05$, Table S3). The number of OTUs and the Shannon, ACE, and Chao indexes of the bacterial community were significantly reduced in the Fo + K29, Fo + 3Y, and Fo + K29 + 3Y treatment groups than in the Fo treatment group, while the Simpson index was markedly increased ($P < 0.05$, Table S4). These results indicated that *T. longibrachiatum* inoculation improved fungal richness, while both *T. longibrachiatum* and *B. stabilis* inoculation reduced bacterial richness and diversity in *F. oxysporum*-infected seedlings.

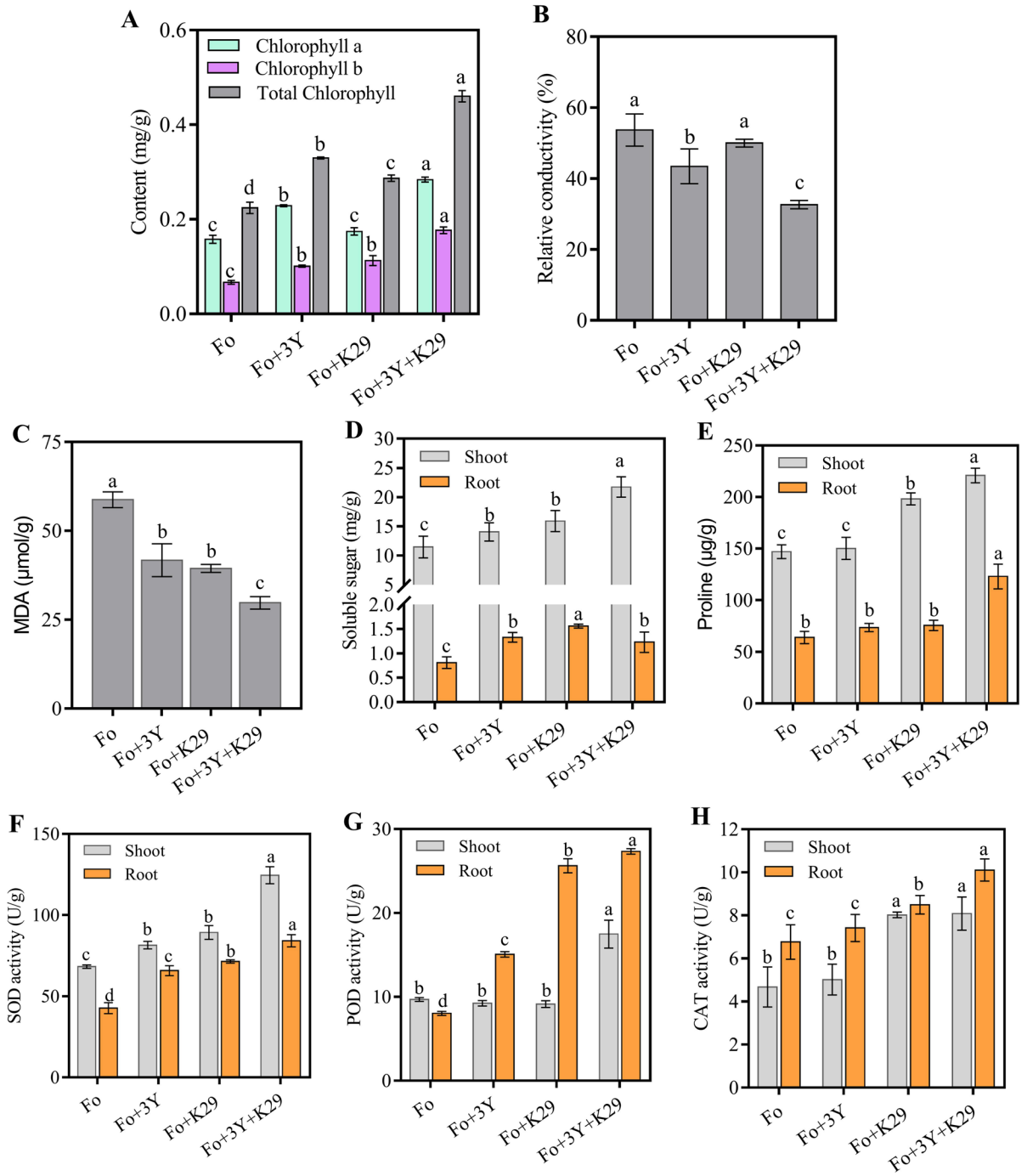

Fig. 5 The effects of different treatment groups on various physiological indicators. **A** Chlorophyll content, **B** Relative conductivity, **C** MDA content, **D** Soluble sugar content, **E** Proline content, **F** SOD activity, **G** POD activity, **H** CAT activity. Fo, plant inoculated with *F. oxysporum*; Fo + 3Y, plant inoculated with *T. longibrachiatum* and *F. oxysporum*; Fo + K29, plant inoculated with *B. stabilis* and *F. oxysporum*; Fo + 3Y + K29, plant inoculated with *F. oxysporum*, *T. longibrachiatum* and *B. stabilis*. Treatment with different strains was used as a variable, shoot or root was analyzed separately by one-way ANOVA. Different letters indicate significant differences at $P \leq 0.05$

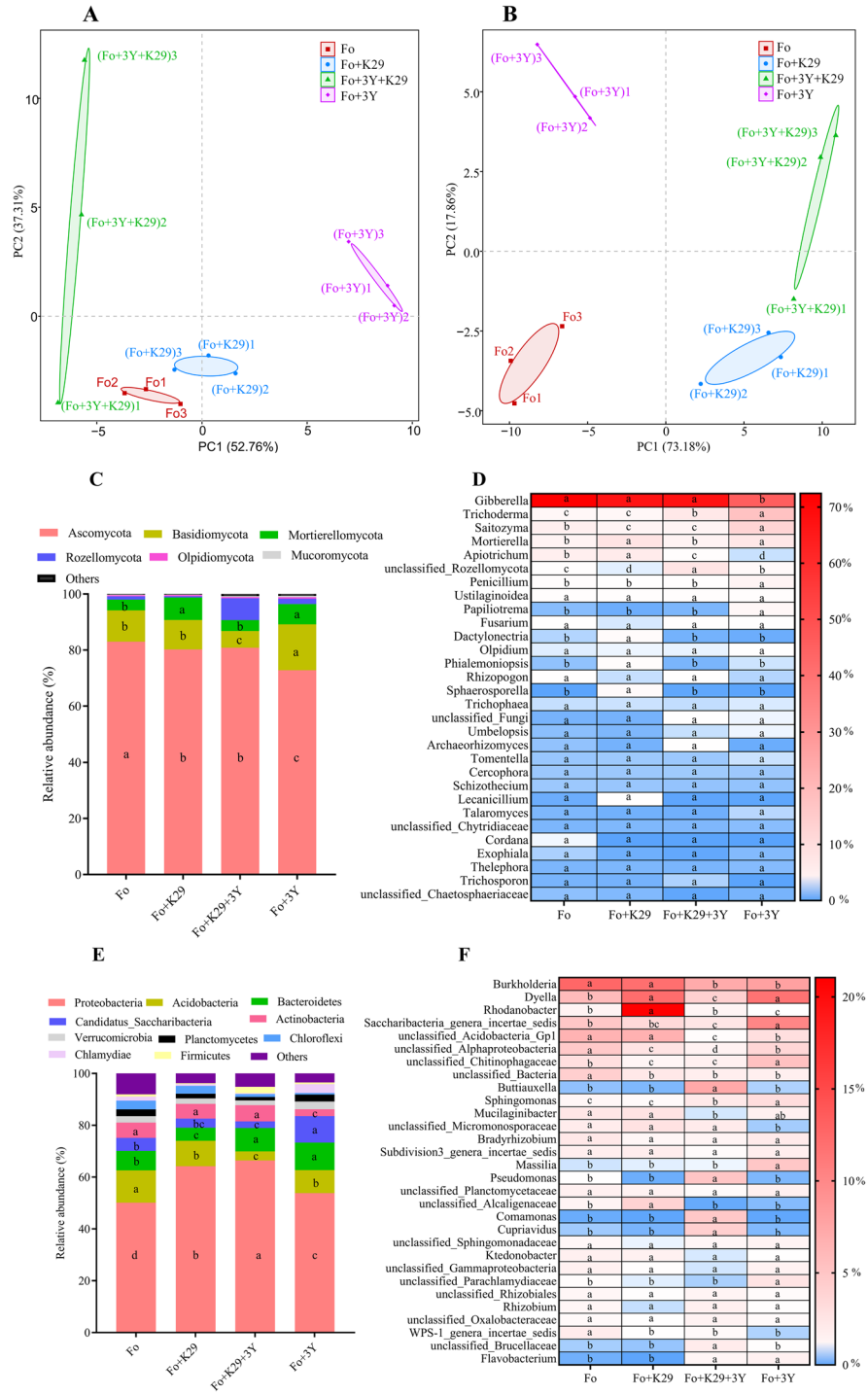

Fig. 6 Rhizosphere soil microbial community composition in different treatments. Principal component analysis (PCA) was used to study the effect of different treatments on the fungal (**A**) and bacterial (**B**) community structure. Relative abundances of the phyla in fungi (**C**) and bacteria (**E**). Heatmaps showing differences in the compositions of the top 30 genera of fungi (**D**) and bacteria (**F**), the heat map was generated from the relative abundance values, and the color change from blue to red suggests an increase in the relative abundance levels. Different letters in each row of the heatmap indicate significant differences at $P \leq 0.05$ among Fo, Fo + K29, Fo + K29 + 3Y, and Fo + 3Y treatments according to Duncan's multiple range test

The rhizosphere soil microbial community composition is shown in Fig. 6. Ascomycota and Basidiomycota were the dominant fungi phyla, with relative abundances of 73–83% and 6–16%, respectively (Fig. 6C). At the top 30 fungal genera, the relative abundance of 19 genera had no significant difference among different treatments (Fig. 6D). Fo + 3Y treatment enhanced the relative abundance of some

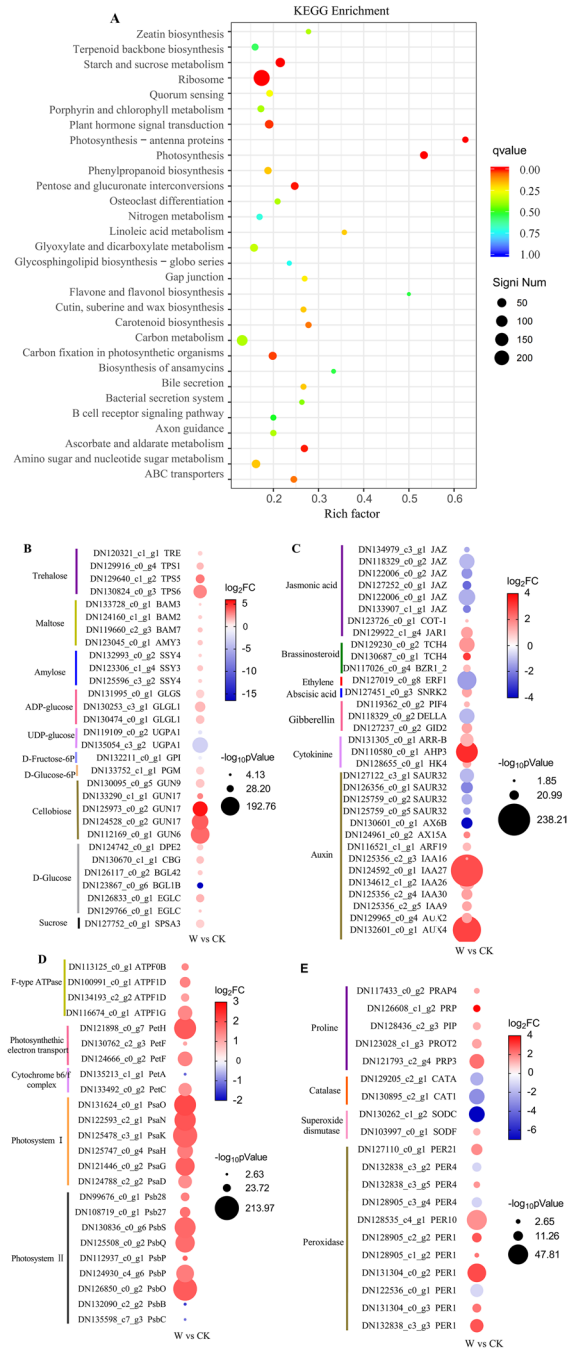

Fig. 7 KEGG analysis and the expression profiles of DEGs involved in key biological pathways associated with plant growth and disease resistance. **A** KEGG enrichment analysis of the DEGs in W vs. CK treatment, the y-axis shows the pathway name, and the x-axis indicates the enrichment factor corresponding to the pathway; the color of the dot represents the q-value, and the size of the dot represents the number of DEGs. **B** DEGs involved in sugar metabolism, **C** DEGs involved in plant hormone signal transduction, **D** DEGs involved in photosynthesis pathway, **E** DEGs involved in antioxidant enzyme activity and proline metabolism; the bubble color was generated from the Log_2 (Fold Change (FC) values) (FC is FPKM [W]/ FPKM [CK]), the color changing from red to blue represents an decrease in the expression levels, and red and blue represents significant up-regulated and down-regulated genes (p Value ≤ 0.05), respectively. The bubble size was generated from -$\log_{10}$ (pValue), the larger the bubble, indicating a higher significant level. CK, seedlings inoculated with *F. oxysporum*; W, seedlings inoculated with *F. oxysporum*, *T. longibrachiatum* and *B. stabilis*

genera, including *Trichoderma*, *Saitozyma*, *Penicillium*, and *Papiliotrema*, K29 and 3Y together caused a marked improvement in the relative abundances of *Trichoderma* and unclassified Rozellomycota ($P < 0.05$, Fig. 6D). The dominant bacteria phyla included Proteobacteria, Acidobacteria, Bacteroidetes, and Actinobacteria; there was a significant increase in the relative abundance of Proteobacteria in response to Fo + K29, Fo + 3Y and Fo + K29 + 3Y compared to Fo treatment ($P < 0.05$, Fig. 6E). Most bacterial genera exhibited significant differences in the relative abundance, some key genera, including *Buttiauxella*, *Sphingomonas*, *Pseudomonas*, *Comamonas*, *Cupriavidus* as well as *Flavobacterium*, were markedly enriched in the Fo + K29 + 3Y treatment group than in the Fo treatment group (Fig. 6F).

Analysis of the KEGG pathway and key DEGs associated with growth and disease resistance

Compared to Fo treatment (CK) alone, there were a total of 8541 DEGs identified in the Fo + 3Y + K29 treatment group (W), of which 4549 were up-regulated and 3992 were down-regulated. These DEGs are enriched in 252 KEGG pathways, eight of which were significantly enriched (q value < 0.05), including ribosome, photosynthesis, photosynthesis-antenna proteins, starch and sucrose metabolism, pentose and glucuronate interconversions, ascorbate and aldarate metabolism, plant hormone signal transduction, and carbon fixation in photosynthetic organisms (Fig. 7A).

The expression profile of DEGs involved in important biological pathways is shown in Fig. 7B-E. Most DEGs involved in sugar metabolism, photosynthesis pathway, peroxidase, superoxide dismutase and proline metabolism were significantly up-regulated (p

value < 0.05, Fig. 7B, D, E). A total of 30 DEGs were shown to participate in starch and sucrose metabolism, and those involved in sucrose, cellobiose, amylose, maltose, and trehalose synthesis were all up-regulated (Fig. 7B). A total of 33 DEGs mapped to the plant hormone signal transduction pathway and shown to be primarily involved in auxin, cytokinin, gibberellin, abscisic acid, ethylene, brassinosteroid, and jasmonic acid metabolism (Fig. 7C). A total of 24 DEGs participated in photosynthesis, 21 of which were up-regulated (Fig. 7D). There were 5 up-regulated DEGs involved in proline metabolism (Fig. 7E); a total of 14 DEGs involved in encoding antioxidant enzymes, including peroxidase (POD), superoxide dismutase (SOD) and catalase (CAT) (Fig. 7E), most DEGs encoding POD and SOD were up-regulated, while two DEGs encoding CAT were all down-regulated, indicating that those DEGs involved in POD and SOD enzyme activities may mainly contribute to regulating the ROS scavenging.

Discussion

The combination of *T. longibrachiatum* and *B. stabilis* effectively controlled *Fusarium* damping-off disease in *P. massoniana*

Damping-off disease caused by *Fusarium* spp. has been widely reported in crops (Scott and Punja 2023) and more recently in pine seedlings, causing serious economic losses (Luo and Yu 2020; Tahat et al. 2021). Biological control products are being extensively developed and applied as an alternative to chemical fungicides (Kim et al. 2021). Scott and Punja (2023) found that five biological-control agents, including *Trichoderma* sp. and *Bacillus* sp., effectively reduced *Fusarium* infection in cannabis (*Cannabis sativa* L.) plants. Our previous study found that *T. koningiopsis* can control *F. oxysporum* damping-off disease in *P. massoniana* seedlings (Yu and Luo 2020). The current study isolated and identified a *T. longibrachiatum 3Y* strain and a *B. stabilis* K29 strain that exhibited plant growth-promoting traits, including potassium dissolution and IAA formation (Luo 2020) and had strong biocontrol activity. To our knowledge, this is the first study to use PGPR (*B. stabilis*) and PGPF (*T. longibrachiatum)* in combination to control damping-off disease in *P. massoniana* seedlings. The combined treatment reduced disease severity by 74%, which was higher than the response elicited by inoculation with a single biological control strain.

Both *T. longibrachiatum* 3Y and *B. stabilis* K29 inhibited the growth of *F. oxysporum*, causing dissolution and deformity of *Fusarium* hyphae. *B. stabilis* K29 has chitinase activity and can secrete proteases that degrade or hydrolyze the cell walls of fungal and fungal-like pathogens (Abdallah et al. 2015). Several beneficial bacteria isolated from various crops are also shown to suppress *Fusarium* growth by secreting cell wall degrading enzymes (Sriwati et al. 2023). Meanwhile, our previous study found that *T. longibrachiatum* 3Y produces various nonvolatile metabolites, including cyclohexanone, alcohols, and organic acids (Luo 2020), which may play key roles in inhibiting *Fusarium* growth. The current study showed that *T. longibrachiatum* and *B. stabilis* can synergize and have a stronger biological effect when used in combination.

T. longibrachiatum and *B. stabilis* impacted the rhizosphere microbial communities of *P. massoniana* against *Fusarium* disease and promoted seedling growth

Rhizosphere microorganisms use several mechanisms to protect plants from pathogen attack (Lee et al. 2021). For instance, the rhizosphere microbial consortium weakens the growth of pathogenic bacteria (Jain and Das 2020), beneficial microorganisms in the rhizosphere can improve disease prevention by enhancing the defense responses of the host (Jain et al. 2015; Jain and Das 2020), and rhizosphere beneficial microorganisms can affect the expression of genes related to stress and disease resistance in plants, dissolve phosphates in soil, and produce substances such as iron carriers, IAA, SA, and extracellular polysaccharides (Wang et al. 2021a). The composition of rhizosphere microbial communities is dependent on the plant species, soil type, and pathogens (Schreiter et al. 2014). *Trichoderma* and *Burkholderia* are well known for effectively colonizing soil or roots to control the invasion of pathogens into plants, which can impact the rhizosphere microbial community and improve plant disease resistance (He et al. 2018; Arici and Demirtas 2019; Yu and Luo 2020). The current study found that the composition of bacterial communities significantly changed when

F. oxysporum-infected *P. massoniana* seedlings were inoculated with both *T. longibrachiatum* and *B. stabilis*.

In the process of controlling plant diseases, biocontrol strains may directly or indirectly affect the composition of rhizosphere microbial communities. Biocontrol strains may directly impact the growth of rhizosphere soil microorganisms through metabolites, active enzymes, nutrition and spatial competition (Whipps., 2001; Song et al. 2023), or indirectly regulate the growth of them through activating soil nutrients or affecting plant root exudates (Saeed et al. 2021). In this study, Ascomycota and Proteobacteria were the dominant phyla in all treatment groups, broadly corresponding to previously published surveys of soil microbial communities (Mendes et al. 2011). The relative abundance of Ascomycota was lower following *T. longibrachiatum* or *B. stabilis* treatment than *F. oxysporum* treatment, which supports previous findings that Ascomycota is less enriched in *Fusarium* wilt disease-free soil (Zhou et al. 2019). Interestingly, the decreased levels of Proteobacteria were associated with some fungal disease suppression (Shen et al. 2015; He et al. 2018), which contrasts with current findings that combined *T. longibrachiatum* and *B. stabilis* treatment significantly increased the abundance of Proteobacteria. These results suggest that Proteobacteria may help to protect *P. massoniana* seedlings against *Fusarium* infection. Meanwhile, we found that there were substantial differences in the relative abundances of most dominant bacterial genera among the four samples, but most fungal genera showed no significant differences. The use of *T. longibrachiatum* or *B. stabilis* increased the abundances of some beneficial microorganisms, including *Sphingomonas*, *Pseudomonas*, *Comamonas* and *Cupriavidus*, most of which are known to improve plant growth during drought, salinity, and oxidative stress (Asaf et al. 2020; Yasmin et al. 2022). However, further experiments are needed to confirm the direct or indirect effects of *T. longibrachiatum* or *B. stabilis* treatment on the relative abundances of those rhizosphere soil microorganisms when *P. massoniana* seedlings against *Fusarium* infection.

T. longibrachiatum and *B. stabilis* treatment changed key physiological pathways of *P. massoniana* seedlings against *F. oxysporum* infection

Plant cells can accumulate reactive oxygen species (ROS) during interactions with potential pathogens, causing oxidative damage, which results in lipid peroxidation and macromolecule break down (Mandal et al. 2008). Malondialdehyde (MDA) is a widely used marker of oxidative lipid injury caused by environmental stress (Kong et al. 2016). The current study found that *F. oxysporum* infection significantly enhanced MDA levels in *P. massoniana* seedlings, while combined *T. longibrachiatum* and *B. stabilis* treatment reduced MDA levels, possibly due to the significant up-regulation of DEGs (*SODF*, *PER4*, *PER1*, etc.) associated with ROS-scavenging enzymes and reduced cell damage (Mandal et al. 2008). These results suggest that the combined use of *T. longibrachiatum* and *B. stabilis* can increase antioxidant enzyme activity (mainly including peroxidase and superoxide dismutase) to help mitigate cell membrane damage caused by *F. oxysporum*.

Sugars are the primary substrates that provide energy and structural material for plant defense responses. They can also act as signaling molecules to activate immune responses against pathogens (Morkunas and Ratajczak 2014). *Trichoderma*-plant-pathogen interactions are associated with an increase in arabinose, xylose, and carbohydrate metabolism, and the higher sugar content in plant tissue improves resistance against *F. oxysporum* (Abdelrahman et al. 2016). The current study identified several up-regulated DEGs associated with sucrose, cellobiose, amylose, maltose, and trehalose metabolism induced by combined *T. longibrachiatum* and *B. stabilis* treatment. The sugars accumulated over time, indicating that their metabolism may play a pivotal role in protecting *P. massoniana* against *F. oxysporum* infection; however, further study is required to verify the mechanism.

Plant hormones modulate the expression of genetic networks involved in defense reactions, of which JA and SA constitute the hormonal backbone of plant immunity (Shigenaga et al. 2017). *Trichoderma* activates ISR through signal transduction pathways activated by JA/ET, but also includes crosstalk with SA and phytohormones associated with plant development (Hermosa et al. 2012). *Trichoderma asperellum* induces systemic resistance in *Arabidopsis thaliana* by activating the expression of genes related to ET, SA, and JA (Huang et al. 2015). Auxin can regulate pathogen resistance (Kazan and Manners 2009) as well as plant lateral root, leaf, flower, and vasculature development. In the present study, many DEGs

associated with JA/auxin signal transduction were activated after inoculation with *T. longibrachiatum* and *B. stabilis*, indicating that JA/auxin pathways may play key roles in reducing *F. oxysporum* infection and promoting *P. massoniana* seedling growth.

Biotic attack from fungal, bacterial, and viral pathogens can decrease the photosynthetic rate and down-regulate photosynthesis-related gene expression (Kangasjärvi et al. 2012). Chlorophyll (Chl) is a vital photosynthetic pigment in plants that greatly influences photosynthetic capacity and plant growth and is easily degraded in response to biotic attack (Bilgin et al. 2010). While chlorophyll content is reduced in *F. oxysporum*-infected tomatoes, levels are significantly increased in the presence of *Arbuscular mycorrhiza* or effective microorganisms (Alshammari et al. 2022). Results from the current study indicate that co-inoculation of *F. oxysporum*-infected *P. massoniana* with *T. longibrachiatum* and *B. stabilis* up-regulates the expression of abundant photosynthetic genes and increases photosynthesis and chlorophyll content, illustrating that the photosynthetic system pathway was activated.

Conclusion

T. longibrachiatum and *B. stabilis* showed antagonistic activity against *F. oxysporum*, effectively controlling *Fusarium* damping-off disease in *P. massoniana* and promoting seedling growth. Combined use of the two biocontrol strains significantly changed the soil bacterial microbial community composition, and affecting the relative abundances of some beneficial microorganisms in the rhizosphere. Meanwhile both biocontrol strains treatment altered plant physiological pathway, and some DEGs associated with growth and disease resistance were up-regulated in response to *Fusarium* infection.

Acknowledgements This work was supported by the National Natural Science Foundation of China (grant number 32160375).

Author contributions **Cun Yu**: conceptualization, data curation, formal analysis, visualization, funding acquisition, manuscript review, and editing. **Jun Lv**: investigation, data curation, formal analysis, methodology, and software. **Hongyun Xu**: conceptualization, data curation, writing the original draft.

Data availability All data generated or analyzed during this study are included in this published article. In addition, sequencing data were deposited to NCBI database.

Declarations

Conflict of interest The authors declare that they have no known competing financial interests or personal relationships that could have appeared to influence the work reported in this paper.

References

Abdallah RAB, Hayfa JK, Sonia MT, Ahlem N, Sined MS, Mejda DR (2015) Endophytic *Bacillus* spp. from wild solanaceae and their antifungal potential against *Fusarium oxysporum* f. sp. lycopersici elucidated using whole cells, filtrate cultures and organic extracts. J Plant Pathol Microbiol 1:6–11. https://doi.org/10.4172/2157-7471.1000324

Abdelrahman M, Abdel-Motaal F, El-Sayed M, Jogaiah S, Shigyo M, Ito SI, Tran LP (2016) Dissection of *Trichoderma longibrachiatum*-induced defense in onion (*Allium cepa* L.) against *Fusarium oxysporum* f. sp. cepa by target metabolite profiling. Plant Sci 246:128–138. https://doi.org/10.1016/j.plantsci.2016.02.008

Alshammari N, Bairum RS, Sulieman AME, Jamal A, Alamoudi M, Elamin HB, Veettil VN (2022) Control of tomato wilt disease fungus fusarium oxysporum f.sp. Lycopersicon by single or combine interaction of mycorrhiza, Trichoderma Harzianum, and effective microorganisms(Microbial Blend). J Pure Appl Microbio 16.https://doi.org/10.22207/JPAM.16.2.64

Arici SE, Demirtas AE (2019) The effectiveness of rhizosphere microorganisms to control Verticillium wilt disease caused by Verticillium dahliae Kleb. in olives. Arab J Geosci 12:781. https://doi.org/10.1007/s12517-019-4962-3

Asaf S, Numan M, Khan AL, Al-Harrasi A (2020) Sphingomonas: from diversity and genomics to functional role in environmental remediation and plant growth. Crit Rev Biotechnol 40:138–152. https://doi.org/10.1080/07388551.2019.1709793

Bagyalakshmi B, Ponmurugan P, Balamurugan A (2017) Potassium solubilization, plant growth promoting substances by potassium solubilizing bacteria (KSB) from southern Indian tea plantation soil. Biocatal Agric Biotechnol 12:116–124. https://doi.org/10.1016/j.bcab.2017.09.011

Bell DK, Well HD, Markham CR (1982) In vitro antagonism of Trichoderma species against six fungal plant pathogens. Ecol Epidemiol 72:379–382. https://doi.org/10.1094/Phyto-72-379

Beneduzi A, Ambrosini A, Passaglia LM (2012) Plant growth-promoting rhizobacteria (PGPR): their potential as antagonists and biocontrol agents. Genet Mol Biol 35:1044–1051. https://doi.org/10.1590/s1415-47572012000600020

Bilgin DD, Zavala JA, Zhu J, Clough SJ, Ort DR, Delucia EH (2010) Biotic stress globally downregulates photosynthesis genes. 33:1597–1613. https://doi.org/10.1111/j.1365-3040.2010.02167.x

Boamah S, Zhang S, Xu B, Li T, Calderón-Urrea A (2021) *Trichoderma longibrachiatum* (TG1) enhances wheat seedlings tolerance to salt stress and resistance to *Fusarium pseudograminearum*. Front Plant Sci 12:741231. https://doi.org/10.3389/fpls.2021.741231

Díaz-Gutiérrez C, Arroyave C, Llugany M, Poschenrieder C, Martos S, Peláez C (2021) *Trichoderma Asperellum* as a preventive and curative agent to control *Fusarium* wilt in *Stevia rebaudiana*. Biol Control 155:104537. https://doi.org/10.1016/j.biocontrol.2021.104537

Dini-Andreote F (2020) Endophytes: the second layer of plant defense. Trends Plant Sci 25:319–322. https://doi.org/10.1016/j.tplants.2020.01.007

Draper HH, Squires EJ, Mahmoodi H, Wu J, Agarwal S, Hadley M (1993) A comparative evaluation of thiobarbituric acid methods for the determination of malondialdehyde in biological materials. Free Radical Bio Med 15:353–363. https://doi.org/10.1016/0891-5849(93)90035-S

Edgar RC (2010) Search and clustering orders of magnitude faster than BLAST. Bioinformatics 26:2460–2461. https://doi.org/10.1093/bioinformatics/btq461

Elshahawy IE, El-Mohamedy RS (2019) Biological control of Pythium damping-off and root-rot diseases of tomato using Trichoderma isolates employed alone or in combination. J Plant Pathol 101:597–608. https://doi.org/10.1007/s42161-019-00248-z

Esmaeel Q, Jacquard C, Sanchez L, Clément C, Barka EA (2020) The mode of action of plant associated *Burkholderia* against grey mould disease in grapevine revealed through traits and genomic analyses. Sci Rep 10:1–14. https://doi.org/10.1038/s41598-020-76483-7

Essalimi B, Esserti S, Rifai LA et al (2022) Enhancement of plant growth, acclimatization, salt stress tolerance and verticillium wilt disease resistance using plant growth-promoting rhizobacteria (PGPR) associated with plum trees (*Prunus domestica*). Sci Hortic 291:110621. https://doi.org/10.1016/j.scienta.2021.110621

Fan L, Zheng S, Wang X (1997) Antisense suppression of phospholipase D alpha retards abscisic acid- and ethylene promoted senescence of Postharvest *Arabidopsis* leaves. Plant Cell 9:2183–2196. https://doi.org/10.1105/tpc.9.12.2183

Grabherr MG, Haas BJ, Yassour M, Levin JZ, Thompson DA, Amit I et al (2011) Full length transcriptome assembly from RNA-Seq data without a reference genome. Nat Biotechnol 29:644–652. https://doi.org/10.1038/nbt.1883

He L, Ye J, Wu B, Huang L, Ren J, Wu X (2018) Effects of genetically modified Burkholderia Pyrrocinia JK-SH007E1 on soil microbial community in poplar rhizosphere. For Pathol 48:e12430. https://doi.org/10.1111/efp.12430

Heo AY, Koo YM, Choi HW (2022) Biological control activity of plant growth promoting rhizobacteria *Burkholderia contaminans* AY001 against tomato *fusarium* wilt and bacterial speck diseases. Biology 11:619. https://doi.org/10.3390/biology11040619

Hermosa R, Viterbo A, Chet I, Monte E (2012) Plant-beneficial effects of Trichoderma and of its genes. Microbiology 158:17–25. https://doi.org/10.1099/mic.0.052274-0

Huang Y, Mijiti G, Wang ZY et al (2015) Functional analysis of the class II hydrophobin gene HFB2-6 from the biocontrol agent Trichoderma Asperellum ACCC30536. Microbiol Res 171:8–20. https://doi.org/10.1016/j.micres.2014.12.004

Jain A, Das S (2020) Synergistic consortium of beneficial microorganisms in rice rhizosphere promotes host defense to blight-causing Xanthomonas oryzae pv. oryzae. Planta 252:106. https://doi.org/10.1007/s00425-020-03515-x

Jain A, Singh A, Singh S, Singh HB (2015) Phenols enhancement effect of microbial consortium in pea plants restrains Sclerotinia sclerotiorum. Biol Control 89:23–32. https://doi.org/10.1016/j.biocontrol.2015.04.013

Jogaiah S, Abdelrahman M, Tran LS, Shin-ichi I (2013) Characterization of rhizosphere fungi that mediate resistance in tomato against bacterial wilt disease. J Exp Bot 64:3829–3842. https://doi.org/10.1093/jxb/ert212

Jung BK, Hong SJ, Park GS, Kim MC, Shin JH (2018) Isolation of *Burkholderia cepacian* JBK9 with plant growth-promoting activity while producing pyrrolnitrin antagonistic to plant fungal diseases. Appl Biol Chem 61:173–180. https://doi.org/10.1007/s13765-018-0345-9

Kangasjärvi S, Neukermans J, Li S, Aro EM, Noctor G (2012) Photosynthesis, photorespiration, and light signalling in defence responses. J Exp Bot 63:1619–1636. https://doi.org/10.1093/jxb/err402

Karlicic V, Zlatković M, Jovičić-Petrović J, Nikolić MP, Orlović S, Raičević V (2021) *Trichoderma* spp. from Pine bark and Pine bark extracts: potent Biocontrol agents against Botryosphaeriaceae. Forests 12:1731. https://doi.org/10.3390/f12121731

Kazan K, Manners JM (2009) Linking development to defense: auxin in plant–pathogen interactions. Trends Plant Sci 14:373–382. https://doi.org/10.1016/j.tplants.2009.04.005

Kim YS, Lee Y, Cheon W, Park J, Kwon HT, Balaraju K, Jeon Y (2021) Characterization of Bacillus velezensis AK-0 as a biocontrol agent against apple bitter rot caused by Colletotrichum gloeosporioides. Sci Rep 11626. https://doi.org/10.1038/s41598-020-80231-2

Kim H, Mohanta TK, Park YH, Park SC, Shanmugam G, Park JS, Jeon J, Bae H (2020) Complete genome sequence of the mountain-cultivated ginseng endophyte Burkholderia stabilis and its antimicrobial compounds against ginseng root rot disease. Biol Control 140:104126

Kong W, Liu F, Zhang C et al (2016) Non-destructive determination of Malondialdehyde (MDA) distribution in oilseed rape leaves by laboratory scale NIR hyperspectral imaging. Sci Rep 6:35393. https://doi.org/10.1038/srep35393

Lee SM, Kong HG, Song GC, Ryu CM (2021) Disruption of firmicutes and actinobacteria abundance in tomato rhizosphere causes the incidence of bacterial wilt disease. ISME J 15:330–347. https://doi.org/10.1038/s41396-020-00785-x

Lin L, Sun J, Cui T et al (2020) Selenium accumulation characteristics of *Cyphomandra betacea* (*Solanum betaceum*) seedlings. Physiol Mol Biol Plants 26:1375–1383. https://doi.org/10.1007/s12298-020-00838-7

Liu Y, Wu C, Hu X, Gao H, Wang Y, Luo H, Cai S, Li G, Zheng Y, Lin C, Zhu Q (2020) Transcriptome profiling reveals the crucial biological pathways involved in cold response in Moso bamboo (*Phyllostachys edulis*). Tree Physiol 40:538–556. https://doi.org/10.1093/treephys/tpz133

Love MI, Huber W, Anders S (2014) Moderated estimation of Fold change and dispersion for RNA-seq data with DESeq2. Genome Biol 15:550. https://doi.org/10.1186/s13059-014-0550-8

Luo X (2020) Diversity of endophytic fungi and its biological contron of damping-off in *Pinus massoniana* Guizhou University, 06. https://doi.org/10.27047/d.cnki.ggudu.2020.001866. (in Chinese)

Luo X, Yu C (2020) First report of damping-off disease caused by *Fusarium oxysporum* in *Pinus massoniana* in China. J Plant Dis Protect 127:401–409. https://doi.org/10.1007/s41348-020-00303-3

Mandal S, Mitra A, Mallick N (2008) Biochemical characterization of oxidative burst during interaction between Solanum lycopersicum and Fusarium oxysporum f s.p. Lycopersici. Physiol Mol Plant P 72:56–61. https://doi.org/10.1016/j.pmpp.2008.04.002

Mehmood MA, Hakeem KR, Bhat RA, Dar GH (2021) Pesticide contamination in freshwater and soil Environs: Impacts, threats, and sustainable remediation. Milton: Apple Academic 2021. https://doi.org/10.1201/9781003104957

Mendes R, Kruijt M, de Bruijn I, Dekkers E, van der Voort M, Schneider JHM et al (2011) Deciphering the rhizosphere microbiome for disease-suppressive bacteria. Science 332:1097–1100. https://doi.org/10.1126/science.1203980

Morales-Rodríguez C, Bastianelli G, Aleandri M, Chilosi G, Vannini A (2018) Application of *Trichoderma* spp. complex and biofumigation to control damping-off of *Pinus radiata* D. Don caused by *Fusarium Circinatum* Nirenberg and O'Donnell. Forests 9:421. https://doi.org/10.3390/f9070421

Morkunas I, Ratajczak L (2014) The role of sugar signaling in plant defense responses against fungal pathogens Acta Physiol. Plant 36:1607–1619. https://doi.org/10.1007/s11738-014-1559-z

Quan W, Ding G (2017) Root tip structure and volatile organic compound responses to drought stress in Masson pine (*Pinus massoniana* Lamb). Acta Physiol Plant 39:258. https://doi.org/10.1007/s11738-017-2558-7

Reglinski T, Rodenburg N, Taylor JT, Northcott GL, Ah Chee A, Spiers TM, Hill RA (2012) *Trichoderma atroviride* promotes growth and enhances systemic resistance to Diplodia pinea in radiata pine (*Pinus radiata*) seedlings. For Path 42:75–78. https://doi.org/10.1111/j.1439-0329.2010.00710.x

Roberts WK, Selitrennikoff CP (1988) Plant and bacterial chitinases differ in antifungal activity. Microbiology 134:169–176. https://doi.org/10.1099/00221287-134-1-169

Saeed Q, Xiukang W, Haider FU, Kučerik J, Mumtaz MZ, Holatko J, Naseem M, Kintl A, Ejaz M, Naveed M et al (2021) Rhizosphere bacteria in plant growth promotion, biocontrol, and bioremediation of contaminated sites: a comprehensive review of effects and mechanisms. Int J Mol Sci 22:10529. https://doi.org/10.3390/ijms221910529

Schreiter S, Sandmann M, Smalla K, Grosch R (2014) Soil type dependent rhizosphere competence and biocontrol of two bacterial inoculant strains and their effects on the rhizosphere microbial community of field-grown lettuce. PLoS ONE 9:e103726. https://doi.org/10.1371/journal.pone.0103726

Scott C, Punja ZK (2023) Biological control of Fusarium oxysporum causing damping-off and Pythium myriotylum causing root and crown rot on cannabis (Cannabis sativa L.) plants. Can J Plant Pathol 45:238–252. https://doi.org/10.1080/07060661.2023.2172082

Sharma A, Shukla A, Attri K, Kumar M, Kumar P, Suttee A, Singh G, Barnwal RP, Singla N (2020) Global trends in pesticides: a looming threat and viable alternatives. Ecotoxicol Environ Saf 201:110812. https://doi.org/10.1016/j.ecoenv.2020.110812

Shen Z, Ruan Y, Xue C, Zhang J, Li R, Shen Q (2015) Rhizosphere microbial community manipulated by 2 years of consecutive biofertilizer application associated with banana *Fusarium* wilt disease suppression. Biol Fertil Soils 51:553–562. https://doi.org/10.1007/s00374-015-1002-7

Shigenaga A, Berens M, Tsuda K, Argueso C (2017) Towards engineering of hormonal crosstalk in plant immunity. Curr Opin Plant Bio 38:164–172. https://doi.org/10.1016/j.pbi.2017.04.021

Sofo A, Milella L, Tataranni G (2010) Effects of *Trichoderma harzianum* strain T-22 on the growth of two *Prunus* rootstocks during the rooting phase. J Hortic Sci Biotechnol 85:497–502. https://doi.org/10.1080/14620316.2010.11512704

Song S, Morales Moreira Z, Briggs AL et al (2023) PSKR1 balances the plant growth–defence trade-off in the rhizosphere microbiome. Nat Plants. https://doi.org/10.1038/s41477-023-01539-1

Sriwati R, Maulidia V, Intan N, Oktarina H, Syamsuddin, Khairan K, Skala L, Mahmud T (2023) Endophytic bacteria as biological agents to control Fusarium wilt disease and promote tomato plant growth. 125:101994. https://doi.org/10.1016/j.pmpp.2023.101994

Tahat MM, Dakil A, Alananbeh H, K (2021) First report of damping off disease caused by *Fusarium oxysporum* on *Pinus pinea* in Jordan. Plant Dis 22. https://doi.org/10.1094/PDIS-10-20-2135-PDN

Takishita Y, Charron JB, Smith DL (2018) Biocontrol Rhizobacterium *Pseudomonas* sp. 23s induces systemic resistance in tomato (*Solanum lycopersicum* L.) against bacterial canker *Clavibacter michiganensis* subsp. Michiganensis Front Microbiol 9:2119. https://doi.org/10.3389/fmicb.2018.02119

Toghueo RMK, Eke P, Zabalgogeazcoa I, de Rodríguez-V´asquez B, Nana LW, Boyom FF (2016) Biocontrol and growth enhancement potential of two endophytic *Trichoderma* spp. from *Terminalia catappa* against the causative agent of Common Bean Root Rot (*Fusarium Solani*). Biol Control 96:8–20. https://doi.org/10.1016/j.biocontrol.2016.01.008

Trapnell C et al (2010) Transcript assembly and quantifification by RNA-Seq reveals unannotated transcripts and isoform switching during cell diffffferentiation. Nat Biotechnol 28:511–515

Tuomisto H (2010) A diversity of beta diversities: straightening up a concept gone awry. Part 1. Defining beta diversity as a function of alpha and gamma diversity. Ecography 33:2–22. https://doi.org/10.1111/j.1600-0587.2009.05880.x

Villa-Rodriguez E, Lugo-Enríquez C, Ferguson S, Parra-Cota PI, Cira-Chávez LA, Santos-Villalobos S (2022) *Trichoderma Harzianum* Sensu Lato TSM39: a wheat microbiome fungus that mitigates spot blotch disease of wheat (*Triticum turgidum* L. subsp. durum) caused by *Bipolaris Sorokiniana*. Biolo Control 175:105055. https://doi.org/10.1016/j.biocontrol.2022.105055

Wang C, Li Y, Li M, Zhang K, Ma W, Zheng L, Xu H, Cui B, Liu R, Yang Y, Zhong Y, Liao H (2021a) Functional assembly of root-associated microbial consortia improves nutrient efficiency and yield in soybean. J Integer Plant Biol 63:1021–1035. https://doi.org/10.1111/jipb.13073

Wang H, Liu R, You MP, Barbetti MJ, Chen Y (2021b) Pathogen biocontrol using plant growth-promoting bacteria (PGPR): role of bacterial diversity. Microorganisms 9:1988. https://doi.org/10.3390/microorganisms9091988

Weerapol Y, Nimraksa H, Paradornuwat A, Sriamornsak P (2019) Development of ready-to-use products derived from Bacillus subtilis strain CMs026 for plant disease control. Biocontrol 64:173–183. https://doi.org/10.1007/s10526-019-09929-1

Whipps JM (2001) Microbial interactions and biocontrol in the rhizosphere. J Exp Bot 52:487–511. https://doi.org/10.1093/jexbot/52.suppl_1.487

Wood NJ, Baker A, Quinnell RJ, Camargo-Valero MA (2020) A simple and non-destructive method for chlorophyll quantification of chlamydomonas cultures using digital image analysis. Front Bioeng Biotechnol 8:746. https://doi.org/10.3389/fbioe.2020.00746

Yasmin H, Bano A, Wilson NL, Nosheen A, Naz R, Hassan MN, Ilyas N, Saleem MH, Noureldeen A, Ahmad P, Kennedy I (2022) Drought-tolerant Pseudomonas sp. showed differential expression of stress-responsive genes and induced drought tolerance in Arabidopsis thaliana. Physiol Plant 174:e13497. https://doi.org/10.1111/ppl.13497

Yu C, Luo X (2020) *Trichoderma Koningiopsis* controls *Fusarium oxysporum* causing damping-off in *Pinus massoniana* seedlings by regulating active oxygen metabolism, osmotic potential, and the rhizosphere Microbiome. Biol Control 150:104352. https://doi.org/10.1016/j.biocontrol.2020.104352

Zhou D, Jing T, Chen Y, Wang F, Qi D, Feng R, Xie J, Li H (2019) Deciphering microbial diversity associated with Fusarium wilt-diseased and disease free banana rhizosphere soil. BMC Microbiol 19:161. https://doi.org/10.1186/s12866-019-1531-6